J|A|C|S
ARTICLES
Published on Web 08/30/2002

Conformational and Spectroscopic Analysis of the Tyrosyl Radical Dipeptide Analogue in the Gas Phase and in Aqueous Solution by a Density Functional/Continuum Solvent Model

Emma Langella,[†] Roberto Improta,[‡] and Vincenzo Barone*[,†]

Contribution from the Dipartimento di Chimica, Università Federico II, via Cintia, I-80126 Napoli, Italy, and Istituto di Biostrutture e Bioimmagini-CNR, Via Mezzocannone 6, I-80134, Napoli, Italy

Received April 1, 2002

Abstract: The conformational and spectroscopic properties of the tyrosyl radical dipeptide analogue (T(R)-DA) are investigated both in gas phase and in aqueous solution by means of density functional calculations. Electronic interactions between backbone and side chain, determining the relative stability of the different energy minimums, depend on the electronic state of the phenoxy substituent. As a consequence, (i) the conformational behavior of T(R)DA is quite different from that of the tyrosine dipeptide analogue, and (ii) the energy required for the homolytic breaking of the OH bond depends on the adopted conformation. The calculated hyperfine coupling constants are in good agreement with the available experimental results. Side-chain−backbone interactions cause an asymmetrization of the magnetic properties of the phenoxy ring and deviations from McConnell relationship. Solvent effects, taken into account by means of a combined discrete/continuum model, significantly affect both the conformational and the magnetic behavior of T(R)-DA.

Introduction

As has been well documented in the past few years, amino acid radicals play an essential role in the catalytic reactions of numerous enzymes.[1,2] Tyrosyl free radicals, in particular, are the active species in metalloenzymes such as galactose oxidase,[3] ribonucleotide reductase (RNR),[4] photosystem II (PSII),[5] and prostaglandin H synthase (PHS).[6] The relative ease by which the tyrosine phenol group can be oxidized and the potential for modulation of the chemical and redox properties of the resulting radical most likely account for its widespread occourrence as a catalytically important paramagnetic species.

In the past decade, tyrosyl radical has been extensively studied by spectroscopic tecniques[7] in a number of enzymatic systems (e.g., RNR,[8] PSII,[9] and PHS[10]) and in simple model systems.[11−16] Recently, thanks to high-frequency electron spin resonance (ESR) spectrometers, it has been possible to resolve the *g*-anisotropy. In particular, it has been demonstrated that the *g*-values are sensitive to the electrostatic environment of tyrosyl radicals.[17−19] However, despite the biological relevance of tyrosyl radical and the large amount of experimental work devoted to its spectroscopic study, a thourough quantum mechanical study of this compound is, to the best of our knowledge, still lacking, since theoretical studies have been limited to phenoxyl-like compounds, without taking into account the peptide backbone.[20−24]

So we have performed a fully ab initio conformational study of the dipeptide analogue of tyrosyl radical (T(R)DA; see Figure

* Author to whom correspondence should be addressed. E-mail: enzo@chemistry.unina.it.
[†] Università Federico II.
[‡] Istituto di Biostrutture e Bioimmagini-CNR.

(1) Stubbe, J. *Annu. Rev. Biochem.* **1989**, *58*, 257−285.
(2) Stubbe, J.; van der Donk, W. A. *Chem. Rev.* **1998**, *98*, 705−762.
(3) Whittaker, M. M.; Whittaker, J. W. *J. Biol. Chem.* **1990**, *265*, 9610−9613.
(4) Sjöberg, B.-M.; Gräslund, A. *Adv. Inorg. Biochem.* **1983**, *5*, 87−110.
(5) Barry, B. A.; Babcock, G. T. *Proc. Natl. Acad. Sci. U.S.A.* **1987**, *84*, 7099−7103.
(6) Smith, W. L.; Eling, T. E.; Kulmacz, R. J.; Marnett, L. J., Tsai, A. L. *Biochemistry* **1992**, *31*, 3−7.
(7) Weil, J. A.; Bolton, J. R.; Wertz, J. E. *Electron paramagnetic resonance: elementary theory and practical applications*; New York: Wiley: 1994. (b) Saifutdinov, R. G.; Larina, L. I.; Vakul'skaya, T. I.; Voronkov, M. G. *Electron paramagnetic resonance in biochemistry and medicine*; Kluwer Academic/Plenum: New York, 2001.
(8) (a) Bender, C. J.; Sahlin, M.; Babcock, G. T.; Barry, B. A.; Chandrashekar, T. K.; Salowe, S. P.; Stubbe, J.; Lindström, B.; Petersson, L.; Ehrenberg, A.; Sjöberg, B.-M. *J. Am. Chem. Soc.* **1989**, *111*, 8076−8083. (b) Hoganson, C. W.; Sahlin, M.; Sjöberg, B.-M-; Babcock, G. T. *J. Am. Chem. Soc.* **1996**, *118*, 4672−4679. (c) van Dam, P. J.; Willems, J. P.; Schmidt, P. P.; Pötsch, S.; Barra, A. L.; Hagen, W. R.; Hoffman, B. M.; Andersson, K. K.; Gräslund, A. *J. Am. Chem. Soc.* **1998**, *120*, 5080.
(9) (a) Hoganson, C. W.; Babcock, G. T. *Biochemistry* **1992**, *31*, 11874−11880 (b) Rigby, S. E. J.; Nugent, J. H. A.; O'Malley, P. J. *Biochemistry* **1994**, *33*, 1734−1742 (c) Warncke, K.; Babcock, G. T.; McCracken, J. *J. Am. Chem. Soc.* **1994**, *116*, 7332−7340. (d) Allard, P.; Barra, A. L.; K. K.; Schmidt, P. P.; Atta, M.; Graeslund, A. *J. Am. Chem. Soc.* **1996**, *118*, 895.
(10) Shi, W.; Hoganson, M. E.; Bender, C. J.; Babcock, G. T.; Palmer, G.; Kulmacz, R. J.; Tsai, A.-l. *Biochemistry* **2000**, *39*, 4112−4121.
(11) Hulsebosch, R. J.; van der Brinck, J. S.; Nieuwenhuis, S. A. M.; Gast, P.; Raap, J.; Lugtemburg, J.; Hoff, A. J. *J. Am. Chem. Soc.* **1997**, *119*, 8685−8694.
(12) Sealy, R. C.; Harman, L.; West, R. R.; Mason, R. P.; *J. Am. Chem. Soc.* **1985**, *107*, 3401−3406.
(13) Barry, B. A.; El-Deeb, M. K.; Sandusky, P. O.; Babcock, G. T. *J. Biol. Chem.* **1990**, *265*, 20139−20143.
(14) Fassanella, E. I.; Gordy, W. *Proc. Natl. Acad. Sci. U.S.A.* **1969**, *62*, 299−304.
(15) Warnke, K.; McCracken, J. *J. Chem. Phys.* **1995**, *106*, 6829−6840.
(16) Mezzetti, A.; Maniero, A. L.; Brustolon, M.; Giacometti, G.; Brunel, L. C. *J. Phys. Chem. A* **1999**, *103*, 9636−9643.
(17) Un, S.; Tang, X.-S.; Diner, B. A. *Biochemistry* **1996**, *35*, 679−684.
(18) Ivancich, A.; Mattioli, T. A.; Un, S. *J. Am. Chem. Soc.* **1999**, *121*, 5743−5753.
(19) Un, S.; Gerez, C.; Elleingand, E.; Fontecave, M. *J. Am. Chem. Soc.* **2001**, *123*, 3048−3054.

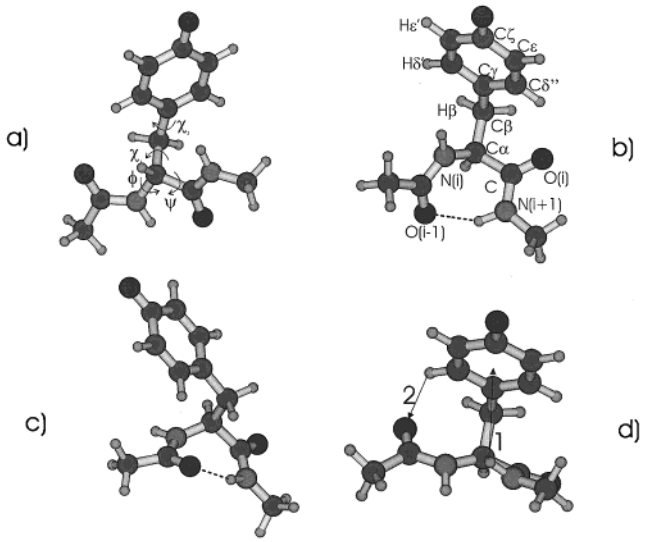

Figure 1. Equilibrium energy structure and atom labeling of four different conformers of T(R)DA: (a) β(a); (b) γ_L(g+); (c) γ_D(g−); (d) δ_L(g+).

1) taking into account the mutual influence between ring and backbone geometric parameters.

Many of the reactions in which tyrosyl radical is involved in enzymatic systems are tuned by the orientation of the aromatic ring with respect to the electron donor (acceptor) species, and thus, it is worth investigating how this orientation is affected by the backbone conformation, at least at a local level. A comparison between the conformational behavior of the tyrosine dipeptide analogue (TDA)[25] and of its radical counterpart (T(R)-DA) (obtained by homolytic breaking of the OH bond) will allow a comprehensive analysis of electronic effects on the conformational behavior of prototype biomolecules. The first goal of the present study is thus to understand how hydrogen atom abstraction from the phenol ring could affect the local conformational behavior of a protein, both from the energetic and from the structural point of view.[26]

We will also present a complete characterization of the hyperfine couplings of T(R)DA, switching on and off a number of environmental effects, to clarify the correlations existing between electronic structure and geometric and spectroscopic parameters. A theoretical characterization of the spectroscopic behavior of aromatic free radicals has been recently performed by one of us on the simple phenoxy radical[27,28] reproducing and explaining the "odd alternant" spin distribution[29] along the aromatic phenoxy ring. In the present study, we will show that the simple model of phenoxy ring is not sufficent to explain the spectroscopic behavior of the tyrosyl radical.

Furthermore, from the methodological point of view, it is worthwhile to validate the computational protocol we have emploied here, to allow a safer use for the study of other relevant biological radicals.

Finally, we will analyze how solvent influences the conformational and spectroscopic properties of T(R)DA. When biological systems are studied, whose natural environment is an aqueous solution, it is indeed very important to take into account solvent effects as well, since they often play a relevant role in determining the physicochemical properties. In the present paper, solvent effects have been taken into account by means of our most recent version of the polarizable continuum model (PCM),[30] whose reliability for conformational and spectroscopic studies of biomolecules in aqueous solution is well documented.[31,32]

Methods

All the calculations were carried out by a development version of the Gaussian package.[33] DFT calculations were performed at the PBE0 level[34] and using the 6-31G(d), 6-31+G(d,p), and EPR-II basis sets.[34−36] Solvent effects have been taken into account by the PCM.[37] In this method, the solvent is represented by an infinite dielectric medium characterized by the relative dielectric constant of the bulk (78.39 for H_2O at 25 °C and 1 atm). A molecular-shaped cavity contains the system under study (the solute plus, possibly, a small number of solvent molecules strongly interacting with it), and its surface separates it from the surrounding solvent. The cavity is built by a new version of the GePol procedure and is composed by interlocking spheres centered on non-hydrogen atoms with radii obtained by the UAHF model.[38] The free energy of solvation (ΔG_{solv}) includes electrostatic, dispersion/repulsion and cavitation contributions

$$\Delta G_{solv} = \Delta G_{el} + \Delta G_{dr} + \Delta G_{cav} \quad (1)$$

In this work, we have used the CPCM[39] variant of PCM that, employing conductor rather than dielectric boundary conditions, allows a more robust implementation. Analytic energy first and second derivatives allow for geometry optimizations and harmonic frequency calculations

(20) (a) Engström, M.; Himo, F.; Gräslund, A.; Minaev, B.; Vahtras, O.; Agren, H. *J. Phys. Chem. A* **2000**, *104*, 5149−5153 (b) Himo, F.; Graslund, F. A.; Eriksson, L. A. *Biophys. J.* **1997**, *72*, 1556.
(21) O'Malley, P. J.; Ellson, D. *Biochim. Biophys. Acta* **1997**, *1320*, 65−72.
(22) Wise, K. E.; Brett Pate, J.; Wheeler, R. A. *J. Phys. Chem. B* **1999**, *103*, 4764−4772.
(23) Boulet, A. M.; Walter, E. D.; Schwartz, D. A.; Gerfen, G. J.; Callis, P. R.; Singel, D. J. *Chem. Phys. Lett.* **2000**, 108−114.
(24) Qin, Y.; Wheeler, R. A.; *J. Chem. Phys.* **1995**, *102*, 1689−1698.
(25) Langella, E.; Rega, N.; Improta, R.; Crescenzi, O.; Barone, V. *J. Comput. Chem.* **2002**, *23*, 650.
(26) Warncke, K.; Perry, M. S. *Biochim. Biophys. Acta* **2001**, *1545*, 1−5.
(27) Adamo, C.; Subra, R.; Di Matteo, A.; Barone, V. *J. Chem. Phys.* **1998**, *109*, 10244−10254.
(28) Adamo, C.; Barone, V.; Subra, R. *Theor. Chem. Acc.* **2000**, *104*, 207−209.
(29) Salem, L. *Molecular Orbital Theory of Conjugated Systems*; W. A. Benjamin, Inc.: New York, 1966.
(30) Rega, N.; Cossi, M.; Scalmani, G.; Barone, V. *J. Chem. Phys.* **2001**, *134*, 7550.
(31) (a) Rega, N.; Cossi, M.; Adamo, C.; Barone, V. In *Theoretical Biochemistry: Processes and Properties of Biological Systems*; Eriksson, L., Ed.; Elsevier: Amsterdan, 2001; pp 467−538. (b) Rega, N.; Cossi, M.; Barone, V. *J. Am. Chem. Soc.* **1997**, *119*, 12962−12967.
(32) (a) Improta, R.; Rega, N.; Aleman, C.; Barone, V. *Macromolecules* **2001**, *134*, 7550. (b) Jolibois, F.; Cadet, J.; Grand, A.; Subra, R.; Barone, V.; Rega, N. *J. Am. Chem. Soc.* **1998**, *120*, 1864. (c) Rega, N.; Cossi, M.; Barone, V. *J. Am. Chem. Soc.* **1998**, *120*, 5723. (d) Nielsen, P. A.; Norrby, P. O.; Liljefors, T.; Rega, N.; Barone, V. *J. Am. Chem. Soc.* **2000**, *122*, 3151.
(33) Gaussian 01, Development Version (Revision B.01). Frisch, M. J.; Trucks, G. W.; Schlegel, H. B.; Scuseria, G. E.; Robb, M. A.; Cheeseman, J. R.; Zakrzewski, V. G.; Montgomery, J. A., Jr.; Kudin, K. N.; Burant, J. C.; Millam, J. M.; Stratmann, R. E.; Tomasi, J.; Barone, V.; Mennucci, B.; Cossi, M.; Scalmani, G.; Rega, N.; Iyengar, S.; Petersson, G. A.; Ehara, M.; Toyota, K.; Nakatsuji, H.; Adamo, C.; Jaramillo, J.; Cammi, R.; Pomelli, C.; Ochterski, J.; Ayala, P. Y.; Morokuma, K.; Salvador, P.; Dannenberg, J. J.; Dapprich, S.; Daniels, A. D.; Strain, M. C.; Farkas, O.; Malick, D. K.; Rabuck, A. D.; Raghavachari, K.; Foresman, J. B.; Ortiz, J. V.; Cui, Q.; Baboul, A. G.; Clifford, S.; Cioslowski, J.; Stefanov, B. B.; Liu, G.; Liashenko, A.; Piskorz, P.; Komaromi, I.; Gomperts, R.; Martin, R. L.; Fox, D. J.; Keith, T.; Al-Laham, M. A.; Peng, C. Y.; Nanayakkara, A.; Challacombe, M.; Gill, P. M. W.; Johnson, B.; Chen, W.; Wong, M. W.;Andres, J. L.; Gonzalez, C.; Head-Gordon, M.; Replogle, E. S.; Pople, J. A. Gaussian, Inc., Pittsburgh, PA, 2001.
(34) Adamo, C.; Barone, V. *J. Chem. Phys.* **1999**, *110*, 6158.
(35) Hariharan, P. C.; Pople, J. A. *Theor. Chim. Acta* **1973**, *23*, 213.
(36) Rega, N.; Cossi, M.; Barone, V. *J. Chem. Phys.* **1996**, *105*, 11060.
(37) (a) Miertuš, S.; Scrocco, E.; Tomasi, J. *Chem. Phys.* **1981**, *55*, 117. (b) Amovilli, C.; Barone, V.; Cammi, R.; Cances, E.; Cossi, M.; Mennucci, B.; Pomelli, C. S.; Tomasi, J. *Adv. Quantum Chem.* **1998**, *32*, 227.
(38) (a) Scalmani, G., Barone, V., submitted. (b) Barone, V.; Cossi, M.; Tomasi, J. *J. Chem. Phys.* **1997**, *107*, 3210.
(39) Barone V.; Cossi, M. *J. Phys. Chem. A* **1998**, *102*, 1995.

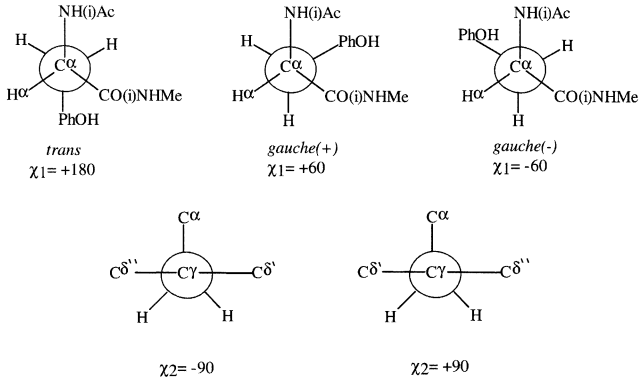

Figure 2. Schematic drawing of the staggered conformers of T(R)DA around χ_1 and χ_2 dihedrals.

in solution.[40] Isotropic hyperfine coupling constants a_N are related to the spin densities at the corresponding nuclei by[41]

$$a_N = \frac{8\pi}{3h} g_e \beta_e g_N \beta_N \Sigma_{\mu,\nu} P^{\alpha-\beta}_{\mu,\nu} \langle \phi_\mu(r) | \delta(r - r_N) | \phi_\nu(r) \rangle \qquad (2)$$

where β_e and β_N, are the electron and nuclear magnetons, respectively, g_e and g_N are the corresponding magnetogyric ratios, h is the Planck constant, $\delta(r)$ is a Dirac delta operator, and $P^{\alpha-\beta}$ is the difference between the density matrices for electrons with α and β spins. In the present work, all the values are given in Gauss (1 G = 0.1 mT), assuming that the free electron g-value is appropriate also for the radicals.

Results and Discussion

We start introducing some nomenclature to facilitate the reading of the following analysis. The general structure of a peptide is defined by the arrangement of the backbone and side-chain dihedral angles: they are shown in Figure 1 together with the atom labeling used in the present work.

As usual in the study of the secondary structure of peptides and proteins, the backbone arrangement is classified with reference to the values of the ϕ,ψ torsional angles, since ω is invariably close to 180° (rarely to 0°). With reference to the staggered conformations around each dihedral angle (gauche, i.e., 60° (g+) or −60° (g−) and antiperiplanar (a), i.e., 180°), nine catchment regions can be defined in the (ϕ,ψ) subspace (the so-called Ramachandran map). These are labeled by the greek letters α (ϕ, $\psi \approx \pm 60°$, $\pm 60°$), β, (ϕ, $\psi \approx 180°$, 180°), γ (ϕ, $\psi \approx$ -60°,±60°), δ (ϕ, $\psi \approx 180°$, ±60°), and ϵ (ϕ, $\psi \approx \pm 60°$, 180°). Enantiomeric pairs are further labeled by L or D subscripts, which are related to the preference observed for L and D residues.

The side-chain orientation is defined by the dihedrals N(i)−C^α−C^β−C^γ (χ_1) and C^α−C^β−C^γ−$C^{\delta 1}$ (χ_2): staggered conformations about both dihedrals are shown in Figure 2.

We have used the geometries of the minimum energy structures found in a recent conformational analysis of TDA[25] as starting points for the radical analogue: the main geometric and energetic parameters of the resulting 18 distinct minimums obtained at the PBE0/6-31G(d) level are listed in Table 1.

Previous conformational studies on dipeptides support the reliability of the geometry optimized at the PBE0/6-31G(d) level.[43] We have thus investigated the energetic effect of basis set extension by single-point PBE0/6-31+G(d,p) computations at PBE0/6-31G(d) geometries. Inspection of Table 1 indicates that the stability order provided by the two basis sets is different. A further extension of the basis set does not change the relative energy ordering for tyrosine-based peptides.[25] Furthermore, the comparison with unrestricted MP2 calculations is biased by large spin contamination usually exhibited by the UMP2 method in open-shell systems. As a consequence, we will refer in the following to PBE0/6-31G(d) results for structural considerations and to more accurate PBE0/6-31+G(d,p) results for energetic considerations.

(1) General Trends in the Gas Phase. The conformational behavior of a peptide radical and of its parent neutral compound can be very different. This is the case, for example, for C^α amino acid radicals, such as the glycine radical.[42]

In the case of tyrosyl, instead, radical formation does not involve backbone in a direct way, the unpaired electron being localized on the side-chain aromatic ring, quite far from the backbone. It could then be expected that the overall conformational behavior of T(R)DA and TDA would be very close.

However, inspection of Table 1 shows that, according to our computations, the conformational behavior of the radical and of its parent neutral molecule exhibits similar general trends, but not negligible differences.

The relative stability of the different conformers of T(R)DA in the gas phase is

$$\beta(a) > \gamma_L(g+) > \delta_L(g+) > \gamma_D(g-) > \alpha_D(g-) > \delta_D(g+) > \epsilon_D(a)$$

This is the same order predicted for TDA, except for the inversion between the two most stable conformers, since in TDA $\gamma_L(g+)$ is slightly more stable than β(a)TDA (vide infra). The β and γ conformers are the most common structures accessible to dipeptide systems:[43,44] the extended backbone typical of β regions allows for a weak intramolecular interaction between polar groups within each residue, while the γ backbone arrangement allows for an intramolecular H bond between carbonyl ($CO_{(i-1)}$) and amino ($NH_{(i+1)}$) groups. α and δ conformers are less common for short chains and generally correspond to high-energy minimums, because the stabilizing interactions in longer chains, like the hydrogen bond patterns, are lacking.

As already found for TDA, our computations predict that the side-chain orientation gives a marked contribution to the whole conformational equilibrium of tyrosine-like compounds, modifying the relative ordering and the energy gaps of the different backbone conformers. As a matter of fact, (1) χ_1 induces more or less marked changes on (ϕ,ψ) and viceversa, and a definite preferred ring orientation within each (ϕ,ψ) conformer. (2) The

(40) Barone V.; Cossi, M. *J. Chem. Phys.* **1998**, *109*, 6246.
(41) Weltner, W. *Magnetic Atoms and Molecules*; Dover: New York, 1989.
(42) Barone, V.; Adamo, C.; Grand, A.; Brunel, Y.; Fontecave, M.; Subra, R. *J. Am. Chem. Soc.* **1995**, *117*, 1083−1089.
(43) (a) Kaschner R.; Hohl, D. *J. Phys. Chem. A* **1998**, *102*, 5111. (b) Beachy, M. D.; Chasman, D.; Murphy, R. B.; Halgren, T. A.; Friesner. R. A. *J. Am. Chem. Soc.* **1997**, *119*, 5908. (c) Improta, R.; Barone, V.; Kudin, K.; Scuseria, G. E. *J. Chem. Phys.* **2001**, *114*, 2541. (d) Improta, R.; Barone, V.; Kudin, K.; Scuseria, G. E. *J. Am. Chem. Soc.* **2001**, *123*, 3311. (e) Improta, R.; Benzi, C.; Barone, V. *J. Am. Chem. Soc.* **2001** *123*, 12568.
(44) (a) Avignon, M.; Huong, P. V.; Lascombe, J. *Biopolymers* **1969**, *8*, 69. (b) Bystrov, V. F.; Portnova, S. L.; Tsetlin, V. I.; Ivanov, V. T.; Ovchinnikov, Y. *Tetrahedron* **1969**, *25*, 493. (c) Benedetti, A.; Di Blasio, B.; Pavone, V.; Pedone, C.; Toniolo, C.; Crisma, M. *Biopolymers* **1992**, *32*, 453. (d) Toniolo, C.; Benedetti, E. In *Molecular Conformation and Biological Interactions: G. N. Ramachandran festschrift*; Balaram, P., Ramaeseshan, S., Eds.; Indian Institute of Science: ??????????, India, 1991.

Table 1. Selected Geometrical Parameters (deg) of Tyrosyl Dipeptide Analogue Optimized at the PBE0/6-31G(d) Level (in the Gas Phase)[a]

	ϕ	ψ	χ_1	χ_2	ΔE	ΔE	ΔE TDA	$\Delta\Delta E$ TDA – T(R)DA
β(a)	−161.6	165.1	−159.7	68.4	0.00[b]	0.00[c]	0.00[d]	0.0
β(g−)	−134.2	153.6	−57.8	96.3	3.24	2.77	3.47	−0.70
β(g+)	−162.6	167.9	58.0	88.5	1.94	1.87	2.40	−0.53
γ_L(a)	−83.4	76.8	−161.9	91.0	0.04	0.26	0.92	−0.66
γ_L(g−)	−84.8	70.3	−56.0	112.1	0.62	0.54	0.85	−0.31
γ_L(g+)	−83.2	57.1	43.2	78.3	−0.52	0.15	−0.23	0.38
γ_D(a)	73.6	−63.8	−171.4	84.9	3.83	3.79	4.39	−0.60
γ_D(g−)	76.4	−54.3	−56.4	99.9	1.68	1.68	2.18	−0.50
γ_D(g+)	58.3	−24.6	72.2	78.3	6.29	6.40	7.51	−1.11
δ_L(a)	−153.7	45.4	−152.7	74.8	3.54	3.86		
δ_L(g−)	−124.9	19.1	−58.6	111.1	3.16	2.77	3.06	−0.23
δ_L(g+)	−126.7	21.4	54.1	83.0	1.16	1.26	1.40	−0.14
α_D(a)	68.2	29.6	−130.9	112.1	6.20	6.35	7.83	−1.48
α_D(g−)	73.7	19.0	−56.4	100.0	3.97	3.90	4.80	−0.90
α_D(g+)	51.9	40.2	51.0	82.3	7.04	7.57	8.74	−1.17
δ_D(a)	−164.1	−44.2	−165.8	78.7	7.98	7.91	8.56	−0.65
δ_D(g+)	−179.2	−28.5	59.9	90.0	5.57	6.02	6.34	−0.32
ϵ_D(a)	63.0	−163.1	−156.1	58.2	7.39	7.43	7.16	0.27

[a] Relative stabilities with respect to β(a) conformers (ΔE in kcal/mol) calculated with 6-31G(d) and 6-31+G(d,p) basis sets on T(R)DA (columns 5 and 6) and calculated with the 6-31+G(d,p) basis set on TDA (column 7) are also reported. Relative stabilities of the different conformers of TDA with respect to the corresponding T(R)DA ones are listed in the last column. [b] Total energy −800.579 023 au. [c] Total energy −800.631 842 au. [d] Total energy −801.274 677 au.

preferred ring orientation is not the same for all the different backbone conformers (the three most stable minimums are in the (g+) and in the (a) arrangement, but the (g−) orientation is preferred by the γ_D and α_D structures). (3) The relative stability of the local energy minimums is strongly influenced by the different ring orientation. In particular, we have, for anti χ_1 regions,

$$\beta > \gamma_L > \gamma_D > \delta_L > \alpha_D > \epsilon_D > \delta_D$$

The β and γ_L conformers are nearly isoenergetic ($\Delta E = 0.26$ kcal/mol), whereas the remaining local minimums are significantly less stable. The stability order becomes

$$\gamma_L > \gamma_D > \delta_L > \beta > \alpha_D \qquad \text{for gauche(−) regions of } \chi_1$$

and

$$\gamma_L > \delta_L > \beta > \delta_D > \gamma_D > \alpha_D \qquad \text{for gauche(+) regions of } \chi_1$$

These results can be rationalized in terms of the steric contacts between the side chain and the backbone and of the NH$\cdots\pi$ interaction.[25] The analysis of the relative stability and the geometry of the energy minimums of T(R)DA shows that ring−carbonyl contacts are essentially repulsive, while $NH_{(i)}$− or $NH_{(i+1)}$−ring contacts are attractive. A more accurate analysis of the combination of these effects in determining the conformational behavior of T(R)DA can be performed along the same lines sketched in our conformational analysis of the parent molecule (TDA).[25]

The same interactions can account also for the main difference between T(R)DA and TDA for what concerns the geometries and relative energies of the minimums. From an energetic point of view, it must be noted that the potential energy surface of the tyrosyl radical is smoother than that of the parent molecule. On one hand, conformations exhibiting one intraresidue N(H)−OC hydrogen bond (β and γ conformers) are relatively destabilized with respect to δ and α conformers. On the other hand, different χ_1 conformers of the same backbone structure are, in general, closer in energy than their TDA analogues. Both these features can be related to the changes of the electronic density of the phenoxy ring due to the abstraction of the hydrogen atom. The SOMO of T(R)DA (which is very similar to the HOMO of TDA) is sketched in Figure 3.

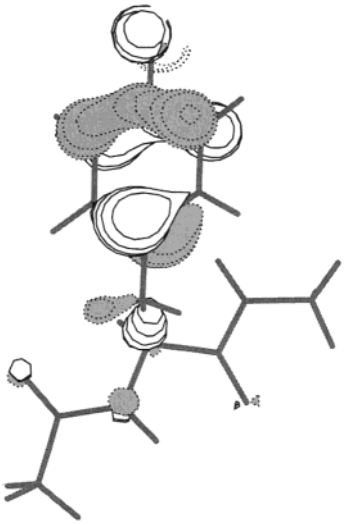

Figure 3. Schematic drawing of the SOMO of T(R)DA.

This is the orbital most involved as the H bond acceptor in the NH−π interaction and in the electronic repulsion with the carbonyl group electron pairs. Both these interactions are weaker in the radical than in its neutral countepart. Due to the formation of the radical, the attractive interaction becomes indeed a "one-electron" instead of a "two-electron" interaction and the repulsive one a "three-electron" instead of a "four-electron" interaction. These differences take account of the smaller dependence on the adopted χ_1 exhibited by T(R)DA.

The decrease in the π electron density of the ring, together with the increase in the electronegativity of the oxygen atom due to the abstraction of the hydrogen atom, leads also to an increase of the polarity of the $C^{\delta}-H^{\delta}$ bonds, as suggested by a slight increase of the charge separation within those bonds

Table 2. Solvation Free Energies (ΔG_{sol} in kcal/mol) of T(R)DA Energy Minimums Obtained at the PBE0/6-31G(d) Level in the Gas Phase[a]

	T(R)DA		TDA	
	ΔG_{sol}	ΔG	ΔG_{sol}	ΔG
β(a)	−12.16	0.0[b]	−13.55	0.0[c]
β(g−)	−16.19	−0.80	−17.86	−0.10
β(g+)	−15.51	−1.41	−17.47	−1.25
γ_L(a)	−12.87	−0.67	−14.86	−0.44
γ_L(g−)	−13.24	−0.45	−14.30	−0.17
γ_L(g+)	−11.20	0.43	−12.42	−0.34
γ_D(a)	−14.25	1.74	−16.34	1.85
γ_D(g−)	−12.98	0.86	−13.90	1.99
γ_D(g+)	−14.20	4.24	−15.36	5.71
δ_L(a)	−15.98	−0.29		
δ_L(g−)	−15.33	0.00	−16.70	0.46
δ_L(g+)	−14.42	−1.10	−15.99	−0.72
α_D(a)	−18.19	0.17	−19.74	1.60
α_D(g−)	−16.45	−0.31	−18.41	0.08
α_D(g+)	−15.53	3.67	−16.81	4.92
δ_D(a)	−16.96	3.18	−19.26	3.24
δ_D(g+)	−14.13	3.60	−15.69	4.03
ϵ_D	−14.54	5.01	−16.04	4.74

[a] Total free energies (ΔG in kcal/mol) relative to the β(a) conformer are also reported. [b] Total free energy = −800.598 399 au. [c] Total free energy = −801.237 202 au.

predicted by Mulliken and natural population analysis.[45] This effect should increase the acid behavior of the H^{δ} atoms, strengthening the nonconventional hydrogen bonds with the carbonyl group (either $CO_{(i)}$ and $CO_{(i-1)}$) that are possible for some conformers. These interactions are operative mainly for the conformers not exhibiting "standard" N(H)−OC intraresidue hydrogen bonds, i.e., δ and α, taking account of the decrease of the energy difference between those structures and the β and γ ones.

The comparison between the relative stability of the different conformers in TDA and T(R)DA allows us to gain some qualitative insight on the effect of the conformation on the energetics of radical formation. Interestingly, the relative dissociation energy for the homolytic cleavage of the OH bond changes by ∼2 kcal/mol within the different conformers (see the last column of Table 1). The formation of the radical seems particularly easy for α_D conformers, whereas OH bond breaking has the highest energetic cost for γ_L conformers.

As could be expected, the most significant structural changes due to the loss of the hydrogen atom involve the phenoxy ring. The $C^{\zeta}-O^{\bullet}$ acquires a double bond character, its bond length decreasing from 1.36 (in TDA) to 1.25 Å, while the $C^{\epsilon}-C^{\zeta}-C^{\epsilon\prime}$ angle (117° in T(R)DA) is narrower than the corresponding one in the closed-shell system (120°), because of the repulsion between the electronic cloud on the phenolic oxygen and that of the CC bond. Interestingly, the $C^{\delta}-H^{\delta}\cdots OC$ interaction is mirrored by the loss of symmetry in the geometry of the phenoxyl ring: the $H^{\delta}-C^{\delta}-C^{\gamma}$ and $H^{\delta\prime}-C^{\delta\prime}-C^{\gamma}$ bond angles are quite different when one of the $H^{\delta}-C^{\delta}$ bonds is in engaged in a nonconventional hydrogen bond. This interaction indeed causes a narrowing by ∼1° of that angle, allowing a closer approach between the groups involved in the hydrogen bond.

Besides the phenoxy ring, the only other relevant structural change due to the formation of the radical concerns the α_L/δ_L area, where there is a shift from $\alpha_L(a)$ to $\delta_L(a)$. The latter

(45) (a) Foster, J. P., Weinhold, F. *J. Am. Chem. Soc.* **1980**, *102*, 7211. (b) Reed, A.; Weinhold, F. *J. Chem. Phys.* **1983**, *78*, 4066. (c) Glendening, E. D.; Weinhold, F. *J. Comput. Chem.* **1998**, *19*, 593.

Table 3. Selected Geometrical Parameters (deg) of Tyrosyl Dipeptide Analogue Optimized at the PBE0-PCM/6-31G(d) Level (in Aqueous Solution)[a]

	ϕ	ψ	χ_1	χ_2	ΔG	ΔG (TDA)
β(g−)	−136.1	161.8	−61.2	99.7	0.34	0.48
γ_L(a)	−84.1	67.8	−172.7	67.8	0.63	0.66
δ_L(g+)	−137.7	24.7	56.2	88.6	0.00[b]	0.00[c]
δ_L(a)	−157.8	36.3	−156.2	68.4	0.57	/
α_L(g−)	−94.8	−0.2	−63.6	114.9	0.32	0.14

[a] Relative stabilities with respect to the minimum energy conformer (ΔG in kcal/mol) calculated at the same level of theory on T(R)DA and TDA (last column) are also reported. [b] Total free energy −800.602 204 au. [c] Total free energy −801.240 602 au.

conformation allows the formation of two hydrogen bonds between the carbonyl and the $C^{\delta}-H^{\delta}$ groups. This interaction also causes a significant deviation of χ_1 from the initial value of 167° (in $\alpha_L(a)$ of TDA) to 150° in the final $\delta_L(a)$ conformer of T(R)DA (see Table 1).

(2) General Trends in Aqueous Solution. Free energy analysis in aqueous solution on structures optimized in the gas phase allows us to investigate the electronic features driving the solute−solvent interaction. Table 2 collects the most important data of the free energy analysis in aqueous solution for the T(R)DA minimums found in the gas phase.

The trend of the solvation energies is very similar to that predicted for TDA: free energy values in solution are closer to each other than the corresponding energies in vacuo. As has long been recognized, the effect of solvation is to flatten out the gas-phase surface, making wider regions accessible.[46−48] A polar solvent indeed reduces the stabilizing effect of all the intraresidue hydrogen bond interactions. For T(R)DA and TDA, this means that not only standard N(H)−OC hydrogen bonds but also N(H)−π interactions are relatively less important, making more similar the energy of both backbone and ring conformers. As a matter of fact, the local contribution of an amidic group to the solvation process is markedly decreased when it is involved in a N(H)$\cdots\pi$ interaction.[25]

Thus, it is not surprising that γ conformers, exhibiting the strongest intraresidue hydrogen bond, are the least stabilized by the solvent. Irrespective of the ring orientation, the stability ordering in aqueous solution of the T(R)DA structures issuing from geometry optimizations in the gas phase is indeed

$$\beta > \delta_L > \gamma_L > \alpha_D > \gamma_D > \delta_D > \epsilon$$

This trend is tha same predicted for TDA, although for that compound the energy differences between the various conformers are usually larger than in T(R)DA. However, this result is not due to the solvent but to the fact that, as outlined above, the potential energy surface in the gas phase is flatter for T(R)DA than for TDA. Variations in the hydration free energy of different conformers can be rationalized in terms of the contributions of polar groups, depending on backbone and side-chain arrangements. The phenoxy oxygen atom gives a strong contribution to the hydration free energy, but this term is nearly constant for all the conformers since the O group never participates in intramolecular interactions and retains the same exposed surface. The situation is different for amidic and

(46) Head-Gordon, T.; Head-Gordon, M.; Frisch, M. J.; Brooks, C. L., III; Pople, J. *J. Am. Chem. Soc.* **1991**, *113*, 5989.
(47) Gould, I. R.; Cornell, W. D.; Hillier, I. H. *J. Am. Chem. Soc.* **1994**, *116*, 9250.
(48) Adamo, C.; Dillet, V.; Barone, V. *Chem. Phys. Lett.* **1996**, *263*, 113.

Table 4. Isotropic Coupling Constants a_N on the Aromatic Ring Atoms of T(R)DA Calculated at PBE0/6-31G(d)//PBE0/Epr-II Level

	$H^{\delta\prime}$	$H^{\delta\prime\prime}$	$H^{\epsilon\prime}$	$H^{\epsilon\prime\prime}$	$H^{\beta\prime}$	$H^{\beta\prime\prime}$	C^{γ}	$C^{\delta\prime}$	$C^{\delta\prime\prime}$	$C^{\epsilon\prime}$	$C^{\epsilon\prime\prime}$	C^{ζ}	O
β(a)	3.38	3.44	−8.11	−7.62	0.77	13.13	13.72	−10.65	−10.27	8.66	8.12	−14.75	−9.26
β(g−)	3.48	3.46	−7.76	−8.13	3.02	7.24	14.11	−10.75	−10.85	8.33	8.72	−14.76	−9.26
β(g+)	3.47	3.46	−7.95	−7.92	4.74	5.54	13.91	−10.67	−10.72	8.51	8.50	−14.80	−9.30
γ_L(a)	3.58	3.44	−7.92	−7.97	4.68	5.30	14.12	−10.57	−10.75	8.49	8.52	−14.80	−9.31
γ_L(g−)	3.41	3.42	−7.56	−8.31	0.68	13.20	13.87	−10.45	−10.88	8.08	8.90	−14.84	−9.31
γ_L(g+)	3.39	3.60	−8.29	−7.62	2.38	9.01	13.96	−10.76	−10.22	8.87	8.16	−14.91	−9.34
γ_D(a)	3.53	3.45	−8.05	−7.87	4.17	6.47	14.04	−10.80	−10.72	8.66	8.44	−14.82	−9.28
γ_D(g−)	3.40	3.44	−7.77	−8.01	2.44	8.03	13.88	−10.53	−10.61	8.29	8.55	−14.75	−9.29
γ_D(g+)	3.45	3.46	−8.07	−7.69	2.19	9.93	14.19	−10.94	−10.54	8.66	8.22	−14.61	−9.19
δ_L(a)	3.49	3.44	−7.93	−7.78	1.55	9.93	14.13	−10.68	−10.52	8.47	8.28	−14.56	−9.26
δ_L(g−)	3.45	3.36	−7.53	−8.26	0.63	13.46	13.85	−10.46	−10.84	8.06	8.82	−14.74	−9.29
δ_L(g+)	3.35	3.51	−8.15	−7.67	3.31	7.65	13.79	−10.64	−10.28	8.69	8.19	−14.81	−9.33
α_D(a)	3.45	3.31	−7.53	−8.12	0.59	13.21	13.85	−10.12	−10.72	7.99	8.63	−14.55	−9.30
α_D(g−)	3.32	3.36	−7.66	−7.98	2.22	9.44	13.74	−10.39	−10.54	8.14	8.49	−14.61	−9.28
α_D(g+)	3.32	3.57	−8.28	−7.42	3.00	8.36	14.19	−10.92	−10.37	8.83	7.95	−14.54	−9.21
δ_D(a)	3.48	3.48	−8.18	−7.71	2.11	9.23	14.01	−10.92	−10.52	8.79	8.24	−14.76	−9.28
δ_D(g+)	3.46	3.37	−7.91	−7.77	4.70	5.97	13.89	−10.52	−10.50	8.45	8.27	−14.67	−9.27
ϵ_D(a)	3.42	3.40	−8.33	−7.50	0.42	18.58	13.69	−10.76	−10.35	8.92	8.03	−14.87	−9.26
exp[a]	1.6	1.6	−6.40	−6.40			9.3	−8.8		2.7	2.7	−9.8	−9.6
exp[b]	1.93		−7.03	−6.24			10[d]						
exp[c]	1.75	1.75	−6.50	−6.50									

[a] Reference 11. [b] Reference 16. [c] Reference 8b. [d] Reference 49.

carbonyl groups, and there is a close parallelism between hydration free energies and exposed surfaces of these groups.

To check the effect of the solvent on the equilibrium geometries, we performed CPCM/PBE0/6-31G(d) geometry optimizations in aqueous solution on some representative T(R)-DA conformers (see Table 3). We selected the three most stable TDA conformers in aqueous solution (δ_L(g+), β(g−), and γ_L-(*a*)), together with some α_L conformers, to verify whether an energy minimum exists for this region in aqueous solution.

Geometry optimization does not significantly affect the stability trend issuing from calculations using the gas-phase geometries: the relative energy ordering between δ_L(g+), β-(g−), and γ_L(*a*) conformers, resulting from both kinds of computations (see the second column of Table 2 and the fifth column of Table 3) is the same and is also similar to that obtained for TDA.

The most significant solvent effect is the stabilization of α conformers. In fact, the δ_L(g−) minimum shifts toward α_L(g−). Solvent does not cause other significant structural changes.

(3) Magnetic properties. In Table 4 are summarized the hyperfine coupling constant (hcc) values computed at the PBE0/6-31G(d)//PBE0/EPR-II level for T(R)DA in the gas phase.

All the computed isotropic hcc's are close to their experimental counterparts, and the agreement is further improved when solvent effect is taken into account (vide infra). The only significant discrepancy involves C^{ϵ} atoms, whose hcc's are remarkably larger than the experimental ones. However, as has already been noted,[21] this result is probably due to an incorrect experimental estimate of the smaller component of the coupling tensor. As a matter of fact, our estimate of the total hyperfine tensor is in agreement with that previously determined on phenoxyl compounds: two components are ∼0 G and one is ∼20 G. This latter value is very close to the experimental estimate (∼19 G).[49] Small errors in the results of the spectral simulations on the two remaining components (−5 G, according to ref 49) can lead to a significant underestimation of the isotropic hcc. An experimental value of 8.1 G is indeed reported for the corresponding carbon atom in phenoxyl radical,[50] supporting the reliability of the above considerations and also the accuracy of our computed hcc's for C^{ϵ} atoms.

Inspection of Table 4 shows that, as previously higlighted, (i) there is an alternation in sign of the hcc's around the aromatic cycle and (ii) a quite large negative hcc is present on ortho and para hydrogens whereas a small positive hcc is present at meta hydrogens. All these effects can be explained by the reminder that two different effects can contribute to the hcc's of a given atom.

The direct (delocalization) contribution arises from the spin density at the nucleus due to the orbital containing the unpaired electron. However, inspection of the SOMO of T(R)DA (see Figure 3) shows that carbon and hydrogen atoms belonging to the phenoxy moiety lie in the nodal plane of the π SOMO; the observed hcc's can thus originate exclusively from spin polarization (Table 4). This contribution takes into account the fact that the unpaired electron interacts differently with the two electrons of a σ spin-paired bond or inner shell, since the exchange interaction is operative only for electrons with parallel spins. This leads to a shorter average distance between electrons with parallel spins than between electrons with antiparallel spins. As a consequence, a positive spin density is induced at each non-hydrogen atom by its own π spin density and a negative spin density is induced at atoms in α positions. This "first-order" contribution takes account of the positive sign of the hcc's of C^{γ} and C^{ϵ} and of the negative sign of the hcc's of H^{ϵ} and C^{δ} atoms. As a matter of fact, C^{δ} atoms not participating to the SOMO do not bear any π spin density.

The presence of a small positive spin density at H^{δ} atoms is thus due to a different ("second-order") contribution, originating from the presence of a large positive spin density on the carbon atom in the β position. Hereafter, to avoid any confusion, we will use latin letters to denote the position with respect the

(49) Hulsebosch, R.J.; van den Brink, J. S.; Hoff, A. J.; Nieuwenhuis, S. A. M.; Rapp, J.; Lugtemburg, J. In *Photosynthesis: From Light to Biosphere*; Mathis, P., Ed.; Kluwer Academic Publishers: Dordrecht, The Netherlands, 1995; Vol. ii, p 255.

(50) Kirste, B. *J. Magn. Reson.* **1982**, *62*, 242.

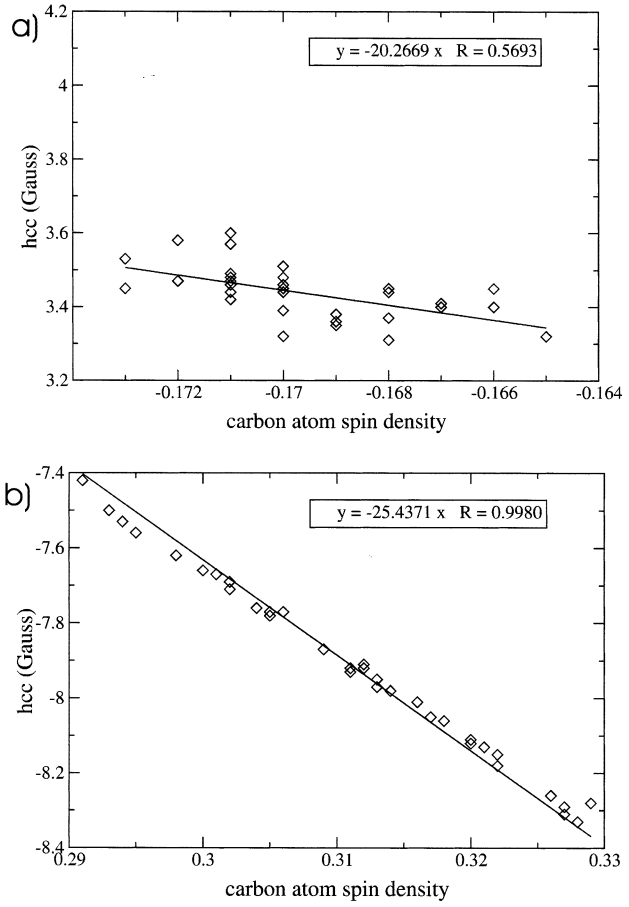

Figure 4. (a) Dependence of the hcc values of δ hydrogens on C^{δ} spin densities for the stable conformers of T(R)DA. (b) Dependence of hcc values of ϵ hydrogens on C^{ϵ} spin densities for the stable conformers of T(R)DA.

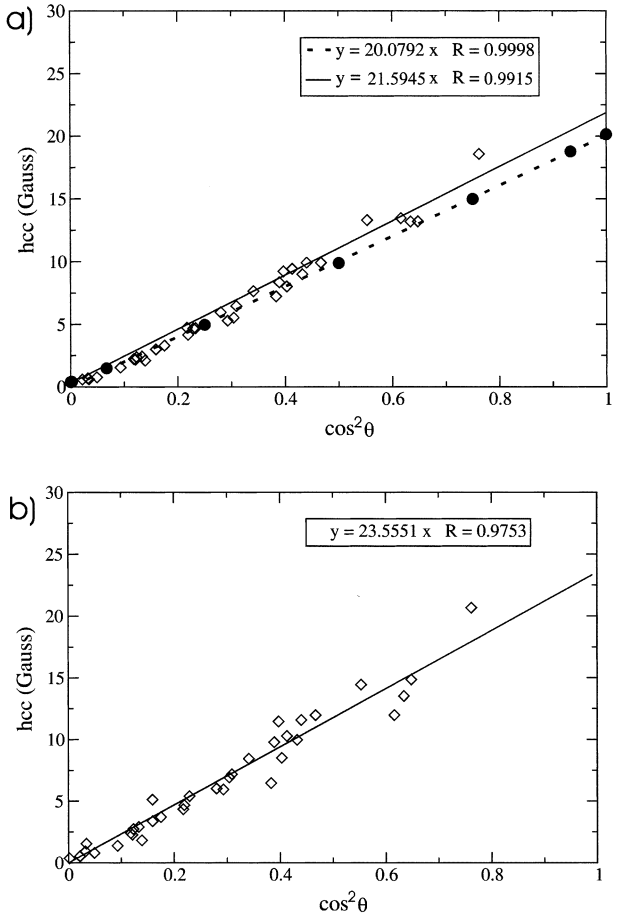

Figure 5. (a) Dependence of a_N values of β-hydrogens on the $\cos^2\theta$ angle for the stable conformers of T(R)DA in the gas phase (open diamonds and continuous line) and for *p*-ethylphenoxy (black circles and dotted line). (b) Dependence of a_N values of β-hydrogens on $\cos^2\theta$ angle for the stable conformers of T(R)DA in aqueous solution.

radical center (**a**, **b**, **c** position for α, β, γ, etc.), leaving the standard peptide notation for the atom labeling within T(R)-DA.

These considerations can be useful when discussing the application of the well-known McConnell[51,52] equation to the calculation of the ring carbon spin density (ρ) starting from the experimental determination of the hydrogen atom hcc's (a_H).

$$a_{H^a} = Q\rho^{C^a} \tag{3}$$

The McConnell equation should strictly be applied only to the hydrogen atom in ortho (H^{ϵ}) position (and to that eventually present in the para position), since only the carbon atom in that position has a nonvanishing π spin density. On the other hand, the value of the H^{δ} hcc's should not be expected to follow the same equation, since they depend from a second-order effect. A plot of the hydrogen atom coupling constants as a function of the calculated spin density of the C^a atoms (see Figure 4a) clearly shows that the predicted *Q* constants are different. For H^{ϵ}, *Q* assumes a value extremely close (−25.4 G) to that previously predicted by the experiments for phenoxyl compounds (−24.9 G)[8a] and the deviations from a linear relationship are small (standard deviation ∼0.1 G). On the contrary, *Q* assumes a significantly smaller value for H^{δ} with a larger standard deviation (∼0.3 G, i.e., ∼10% of the hcc value). The presence of the peptide backbone is mainly responsible for the deviation from a linear behavior of the plot shown in Figure 4a. As a matter of fact, C^{δ} and H^{δ} atoms are the most involved in the backbone−ring interaction, especially in the $C^{\delta}H^{\delta}\cdots OC$ hydrogen bonds.

It is not surprising that the hcc of the H^{δ} atom shows a linear dependence also on the spin density of the C^{δ} atom, since this latter depends to the first order from the spin density of C^{γ} and C^{ϵ} atoms. $a_{H^{\delta}}$ could thus obey a modification of McConnell equation, i.e.:

$$a_{H^{\delta}} = Q_1\rho^{C\gamma} + Q_2\rho^{C\epsilon} \tag{4}$$

The dependence of the H^{δ} hcc's on the spin density of two carbon atoms (those in **b** position), via a likely smaller constant, can lead to some partial error cancellation and to similar values for the *Q* constant. The analysis of the dependence of the H^{β} coupling constants on the χ_2 dihedral allows us to verify the validity of the modification of the McConnell equation relating, for $Ar^{\bullet}-CH_2-R$ systems ($Ar^{\bullet}$ = aryl radical group), the hcc of the hydrogen in **b** position to the spin density of an aromatic carbon atom in **a** position, i.e.

$$a_{H^b} = B\rho^{C^a}\cos^2\theta \tag{5}$$

where θ is the dihedral angle defined by the p_z orbital on the

(51) McConnell, H. M.; Chesnut, D. B. *J. Chem. Phys.* **1958**, *28*, 107.
(52) McConnell, H. M. *J. Chem. Phys.* **1956**, *24*, 764.

Table 5. Isotropic Coupling Constants a_N on the Aromatic Ring Atoms of T(R)DA calculated at the PBE0/6-31G(d)//PBE0-PCM/Epr-II Level

	$H^{\delta\prime}$	$H^{\delta\prime\prime}$	$H^{\epsilon\prime}$	$H^{\epsilon\prime\prime}$	$H^{\beta\prime}$	$H^{\beta\prime\prime}$	C^{γ}	$C^{\delta\prime}$	$C^{\delta\prime\prime}$	$C^{\epsilon\prime}$	$C^{\epsilon\prime\prime}$	C^{ζ}	O
β(a)	3.10	3.05	−7.75	−7.19	0.78	14.04	13.56	−10.17	−9.78	7.74	7.11	−12.59	−9.13
β(g−)	2.98	3.03	−7.13	−7.65	3.19	8.01	13.66	−9.83	−10.12	6.98	7.57	−12.39	−9.12
a	2.92	3.01	−6.97	−7.68	2.47	9.27	13.63	−9.71	−10.12	6.78	7.57	−12.33	−9.18
β(g+)	3.03	3.03	−7.51	−7.39	4.98	6.14	13.48	−9.99	−9.94	7.42	7.30	−12.52	−9.19
γ_L(a)	3.11	3.05	−7.48	−7.44	5.17	5.80	13.79	−9.96	−10.04	7.40	7.35	−12.53	−9.18
a	2.97	3.01	−7.17	−7.43	0.68	14.65	13.92	−9.92	−10.04	6.99	7.34	−12.29	−9.14
γ_L(g−)	3.03	3.12	−7.16	−7.86	0.65	14.11	13.69	−9.85	−10.31	7.05	7.83	−12.62	−9.19
γ_L(g+)	3.15	3.16	−7.88	−7.22	2.54	9.77	13.81	−10.30	−9.74	7.89	7.17	−12.75	−9.21
γ_D(a)	3.09	3.05	−7.60	−7.33	4.41	7.07	13.62	−10.08	−9.94	7.54	7.24	−12.56	−9.16
γ_D(g−)	3.04	3.09	−7.30	−7.66	2.56	8.68	13.67	−9.91	−10.12	7.21	7.61	−12.58	−9.17
γ_D(g+)	2.97	2.94	−7.41	−7.17	2.32	10.85	13.72	−10.03	−9.79	7.27	7.02	−12.18	−9.03
δ_L(a)	2.99	2.95	−7.38	−7.24	1.61	10.99	13.66	−9.90	−9.80	7.25	7.08	−12.21	−9.09
δ_L(g−)	2.98	3.06	−7.05	−7.81	0.60	14.52	13.58	−9.75	−10.24	6.91	7.75	−12.46	−9.15
δ_L(g+)	3.07	3.08	−7.71	−7.28	3.51	8.20	13.59	−10.12	−9.78	7.67	7.19	−12.62	−9.21
a	2.99	3.02	−7.48	−7.28	5.23	5.99	13.56	−9.96	−9.79	7.16	7.37	−12.46	−9.25
α_D(a)	2.92	2.92	−7.01	−7.57	0.54	14.32	13.48	−9.45	−9.97	6.82	7.43	−12.19	−9.13
α_D(g−)	2.97	3.01	−7.18	−7.64	2.27	9.99	13.51	−9.78	−10.07	7.05	7.57	−12.44	−9.15
α_D(g+)	2.95	2.90	−7.74	−6.75	3.24	9.27	13.73	−10.17	−9.48	7.62	6.52	−12.05	−9.01
δ_D(a)	3.05	3.00	−7.64	−7.21	2.25	10.15	13.55	−10.11	−9.78	7.57	7.08	−12.47	−9.15
δ_D(g+)	3.09	3.04	−7.53	−7.40	4.97	6.26	13.65	−10.04	−9.99	7.49	7.33	−12.56	−9.16
ϵ_D(a)	3.15	3.07	−8.03	−7.06	0.39	19.74	13.55	−10.34	−9.77	8.05	7.00	−12.75	−9.15

[a] Isotropic coupling constants computed at the PBE0-PCM/6-31G(d)//PBE0-PCM/EPR-II level.

adjacent carbon on the aromatic ring and the $C^{\beta}-H^{\beta}$ bond. Clearly the θ value is directly related to the χ_2 one, thus explaining the different hcc's found for different χ_2 conformers. A plot of $H^{\beta\prime}$ and $H^{\beta\prime\prime}$ hcc's versus the corresponding $\cos^2\theta$ values for all the conformers accessible to T(R)DA is shown in Figure 5.

Inspection of Figure 5 shows that the relationship between $a_{H^{\beta}}$ and $\cos^2\theta$ is roughly linear, confirming the qualitative validity of the McConnell empirical equation. The value predicted for B (∼54 G by considering an average value of 0.4 for the C^{γ} Mulliken spin density) is in good agreement with that predicted on the basis of the experimental results (58 G).[53] However, not negligible deviations from the McConnell equation are observed for several hydrogen atoms, their relative importance being larger for θ close to 90°. When the H^{β} atoms are close to the ring plane, the spin density has a negligile direct contribution (the one exhibiting the $\cos^2\theta$ dependence) and indirect effects become dominant. The measured hcc's result thus from a delicate balance between second-order polarization effect, giving a positive contribution not depending on θ, and dipolar coupling with C^{γ}.

Furthermore, it is necessary to take into account the effect of small geometry distortions and electronic interactions on the hydrogen spin density due to the presence of the peptide backbone. With the aim to evaluate the role played by these latter effects on the hcc values, we then studied the dependence of the $a_{H^{\beta}}$ values on the θ angle for the model system $Ar^{\bullet}-CH_2-CH_3$. The result is shown in Figure 5b. The comparison between the two graphs in Figure 5 shows that for *p*-ethylphenoxy the deviations from linearity are negligible, thus confirming that the peptide backbone leads to significant differences in the magnetic properties of T(R)DA with respect to simpler model compounds.

Finally, it is worth higlighting that the ring−backbone interactions cause also a non-negligible asymmetrization of the magnetic properties of the ring atoms. $C^{\delta}-H^{\delta}$ moieties, as well as $C^{\epsilon}-H^{\epsilon}$ ones, are no more equivalent, exhibiting differences in the spin densities and in the hcc's close to 10% of their total value.

(4) Environmental Effects on Magnetic Properties. In the final step of our analysis, we evaluated the influence of the solvent on the magnetic properties of T(R)DA, discriminating between direct and indirect solvent effects. The so-called direct solvent effects refer to the polarization of the electron (and spin) distribution due to the solvent reaction field. On the other hand, indirect effects are related to the solute geometry modifications induced by the solvent. The hcc's of all the 18 gas-phase minimums of T(R)DA including only the direct solvent effect (calculated at the PBE0/6-31G(d)//PBE0-PCM/EPR-II level) are listed in Table 5.

A comparison between Tables 4 and 5 shows that direct solvent effects are not negligible: in particular, the absolute value of all the hcc's is decreased, improving the agreement with the avalaible experimental results. This effect is particularly significant for C^{ζ}, whose hcc is decreased by more than 2 G. On the other hand, geometry optimization in aqueous solution leads only to a small variation of the hcc's, suggesting that for T(R)DA indirect solvent effects play a minor role. Furthermore, any indirect solvent effect is due to small changes in the backbone dihedrals, without any remarkable influence on the geometry of the phenoxy moiety. Test calculations on *p*-ethylphenoxy show that the indirect solvent effect is negligible.

Previous computational studies in aqueous solution have shown that the magnetic properties of organic free radicals are influenced not only by bulk solvent effects but also by explicit hydrogen bonds with water molecules of the first solvation shell.[54,55] As a matter of fact, PBE0/6-31+G(d,p) test calculations on the adduct between two water molecules and the T(R)-DA β(a) conformer (see Figure 6) show that the energetic

(53) Fessenden, R. W.; Schuler, R. H. *J. Chem. Phys.* **1963**, *39*, 2142.

(54) Symons, M. C. R.; Pena-Nuñez, A. *J. Chem. Soc., Faraday Trans. 1* **1985**, *81*, 2421.

(55) (a) Improta, R.; Scalmani, G.; Barone, V. *Chem. Phys. Lett.* **2001**, *336*, 349. (b) Rega, N.; Cossi, M.; Barone, V. *J. Chem. Phys.* **1996**, *105*, 11060. (c) Rega, N.; Cossi, M.; Barone, V. *J. Am. Chem. Soc.* **1998**, *120*, 5723. (d) Barone, V.; Bencini, A.; Cossi, M.; di Matteo, A.; Mattesini, M.; Totti, F. *J. Am. Chem. Soc.* **1998**, *120*, 7069.

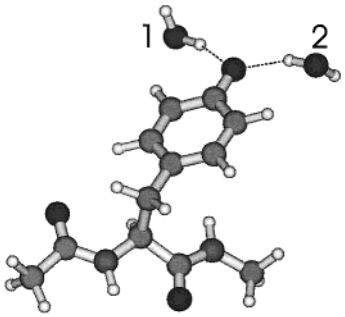

Figure 6. Equilibrium geometry of the adduct between two water molecules and the β(a) conformer of T(R)DA.

stabilization deriving from the coordination of each water molecule to the C−O• moiety is larger by ∼1 kcal/mol than the dimerization energy of two water molecules calculated at the same level of theory (∼7 and ∼6 kcal/mol, respectively). This result suggests that in the calculations of the magnetic properties it is necessary to include two explicit water molecules (see Table 6).

Inclusion of explicit hydrogen-bonded water molecules leads to a decrease of the ring hcc's of the same order of magnitude as that due to bulk solvent effect. The only exception concerns the phenoxy oxygen, whose hcc is slightly increased by the inclusion of explicit water molecules. In general, the agreement with experimental hcc's is better than that obtained by including bulk solvent effect only. Interestingly, applying the McConnell relationship to $a_H\beta$ (see Figure 5b) gives a B value (∼58.7 G) in better agreement with the experimental one (58 G), obtained for aliphatic radicals[53] than that computed in the gas phase (54 G), even if with a larger standard deviation. It is also interesting to highlight that the calculated value for $B\rho^{Ca}$ (∼23.5 G) is in good agreement with that found experimentally[16] for the *N*-acetyl,L-tyrosine radical (∼22.4 G).

As the final step of our analysis of environmental effects, we checked for the effect of an asymmetric hydrogen bond to the C−O• moiety, by performing a PBE0-PCM/EPR-II calculation on the adduct between β(a) T(R)DA and just one water molecule (see Figure 6). Inspection of Table 6 shows that (i) the effect of explicit hydrogen bonds on the magnetic properties of T(R)DA is additive and (ii) the presence of asymmetric hydrogen bonds does not cause any further asymmetrization of the spin properties of the phenoxy ring.

Table 6. Isotropic Coupling Constants a_N on the Aromatic Ring Atoms of T(R)DA Calculated at the PBE0/6-31G(d)//PBE0-PCM/Epr-II Level Including Two Water Molecules in the Solute Description

	$H^{\delta\prime}$	$H^{\delta\prime\prime}$	$H^{\epsilon\prime}$	$H^{\epsilon\prime\prime}$	$H^{\beta\prime}$	$H^{\beta\prime\prime}$	O
β(a)[a]	2.77	2.70	−7.39	−6.79	14.44	0.80	−9.21
	(2.89)	(2.88)	(−7.50)	(−6.99)	(14.13)	(0.82)	(−9.28)
β(g−)	2.62	2.67	−6.76	−7.23	6.47	5.12	−9.18
β(g+)	2.70	2.70	−7.08	−7.11	6.92	4.35	−9.28
γ_L(a)	2.79	2.74	−7.13	−7.08	5.95	5.41	−9.26
γ_L(g−)	2.71	2.81	−6.83	−7.50	13.52	0.93	−9.29
γ_L(g+)	2.85	2.87	−6.87	−7.58	9.98	2.74	−9.30
γ_D(a)	2.77	2.72	−7.24	−6.98	7.19	4.68	−9.25
γ_D(g−)	2.72	2.78	−6.96	−7.31	8.52	2.91	−9.27
γ_D(g+)	2.58	2.60	−6.82	−6.92	11.59	2.28	−9.07
δ_L(a)	2.63	2.59	−6.95	−6.86	11.97	1.39	−9.14
δ_L(g−)	2.62	2.73	−6.67	−7.43	11.98	1.56	−9.22
δ_L(g+)	2.74	2.76	−6.90	−7.37	8.45	3.72	−9.29
α_D(a)	2.55	2.57	−6.61	−7.19	14.86	0.54	−9.20
α_D(g−)	2.62	2.69	−6.80	−7.28	10.29	2.40	−9.24
α_D(g+)	2.46	2.59	−6.24	−7.34	9.79	3.38	−9.03
δ_D(a)	2.73	2.65	−7.30	−6.81	11.47	1.83	−9.23
δ_D(g+)	2.71	2.77	−7.02	−7.19	6.03	5.54	−9.25
ϵ_D(a)	2.86	2.74	−7.73	−6.69	20.67	0.37	−9.26
exp[b]	1.6	1.6	−6.40	−6.40			−9.6
exp[c]	1.93		−7.03	−6.24			
exp[d]	1.75	1.75	−6.50	−6.50			

	C^{γ}	$C^{\delta\prime}$	$C^{\delta\prime\prime}$	$C^{\epsilon\prime}$	$C^{\epsilon\prime\prime}$	C^{ζ}	C^{β}
β(a)[a]	13.34	−9.71	−9.28	6.93	6.27	−10.70	−5.27
	(13.44)	(−9.88)	(−9.53)	(7.28)	(6.65)	(−11.64)	(−5.27)
β(g−)	13.42	−9.33	−9.59	6.18	6.70	−10.48	−5.40
β(g+)	13.21	−9.48	−9.48	6.56	6.59	−10.68	−5.30
γ_L(a)	13.59	−9.53	−9.58	6.63	6.57	−10.69	−5.12
γ_L(g−)	13.49	−9.41	−9.87	6.31	7.03	−10.81	−5.06
γ_L(g+)	13.65	−9.31	−9.91	6.41	7.19	−10.96	−5.14
γ_D(a)	13.38	−9.62	−9.47	6.77	6.47	−10.73	−5.23
γ_D(g−)	13.45	−9.46	−9.67	6.45	6.82	−10.75	−5.16
γ_D(g+)	13.53	−9.29	−9.47	6.23	6.33	−10.25	−5.57
δ_L(a)	13.43	−9.38	−9.29	6.37	6.27	−10.27	−5.16
δ_L(g−)	13.31	−9.23	−9.74	6.11	6.93	−10.59	−5.11
δ_L(g+)	13.37	−9.30	−9.67	6.39	6.90	−10.76	−5.17
α_D(a)	13.21	−8.93	−9.48	5.98	6.59	−10.27	−5.10
α_D(g−)	13.25	−9.28	−9.59	6.25	6.75	−10.56	−5.00
α_D(g+)	13.48	−8.85	−9.66	5.56	6.76	−10.04	−5.50
δ_D(a)	13.33	−9.65	−9.26	6.80	6.25	−10.60	−5.22
δ_D(g+)	13.46	−9.53	−9.59	6.51	6.71	−10.70	−5.17
ϵ_D(a)	13.33	−9.93	−9.29	7.34	6.21	−10.97	−5.25
exp[b]	9.3, 10[e]	−8.8		2.7	2.7	−9.8	

[a] The results in parentheses were obtained with only one explicit water molecule. [b] Reference 11. [c] Reference 16. [d] Reference 8b. [e] Reference 49.

Discussion and Conclusion

Our calculations predict that the potential energy surface of the tyrosine radical dipeptide analogue is smoother than that of the parent molecule, since all the backbone (ϕ and ψ) and ring (χ_1) conformers are closer in energy. Although the formation of the radical involves almost exclusively the side-chain substituent, the conformation of tyrosine is not negligibly altered by the homolytic breaking of the OH bond. Furthermore, the relative energetic cost for this latter reaction depends to some extent on the conformation adopted by the tyrosine residue. Obviously, an accurate determination of the activation energy of the OH bond-breaking reaction is outside the scope of the present paper; however, the predicted energy differences are large enough to be relevant. Can this result be significant for understanding the behavior of tyrosyl radical in proteins?

On one hand, only local effects (though both intrinsic and environmental) have been taken into account in our calculations. Interresidue interactions could obviously deeply influence the behavior of tyrosine (e.g., via the formation of hydrogen bonds involving either the backbone or the phenol OH group). On the other hand, the role of local effects in determining the global structure of proteins has been highlighted.[56] The features evidenced by our calculations could thus be one of the factors, though probably not the most important, influencing the reactivity of tyrosine toward radicals, and some phenomena could be tuned by these effects. Just to give a few examples, they could help in determining which among the different tyrosines of a protein undergoes the radical reaction. Alternatively, they could be relevant in case of "conformationally gated" reactions. Finally, our computations suggest that the relative

(56) (a) Shortle, D. *Protein Sci.* **2002**, *11*, 18. (b) Toth, G.; Murphy, R.; Lovas, S. *Protein Eng.* **2001**, *14*, 543.

orientation between backbone and ring can change after the formation of the radical, and this should be remembered when analyzing the behavior of the radical on the basis of experimental structures containing the neutral residue.[26] For instance, all the conformations allowing for a weak $H^{\delta}\cdots OC$ hydrogen bond are relatively more stable in T(R)DA than in TDA, while the opposite is true for the conformers exhibiting $N(H)\cdots\pi$ interactions.

The backbone−ring interactions play a not negligible role in modulating the magnetic properties of tyrosyl. As a matter of fact, the geometry and electronic structure of the phenoxy ring is no more symmetric, leading to some differences in the spin densities and in the hcc's of atom pairs that are perfectly equivalent in phenoxyl (C^{ϵ} and $C^{\epsilon\prime}$, C^{δ} and $C^{\delta\prime}$, and so on). Some of the "asymmetric" features exhibited by tyrosyl in some protein systems could thus depend on local effects and not, as usually assumed, on an asymmetric environment (electrostatic, hydrogen bonds) experienced by the radical.

The strong correlation between backbone and ring geometric parameters is also relevant for understanding the possible orientation of the phenoxy ring with respect to the protein matrix. This datum is often inferred by the magnetic behavior of H^{β} hydrogens, analyzed in the framework of the modified McConnell equation (eq 3) connecting the hydrogen hcc's to the θ angle between the CH bond and the normal to the ring plane. This angle is obviously related to the χ_2 dihedral, whose optimal value strongly depends on the actual values of backbone and χ_1 dihedrals. The above considerations also suggest some caution when using the McConnell equation for determining the ring orientation. Even if our computations show a rough linear relationship between H^{δ} hcc's and $\cos^2\theta$, there are not negligible deviations from the McConnell equation, mostly (but not only) for hydrogen atoms close to the ring plane. So, using a unique value for the B constant of eq 4 can lead to errors in the determination of the θ angle and, even more, in the estimate of the C^{γ} spin density.

As previously highlighted for phenoxy radical, our calculations show that different physical effects are responsible for the hcc's of the ring proton and any similarity between the Q constant used in eq 3 for δ and ϵ hydrogen atoms should be considered fortuitous.

PCM calculations show that a polar solvent influences both the conformational and the magnetic properties of T(R)DA. The potential energy surface in aqueous solution is indeed flatter than in the gas phase and the absolute value of the ring atoms' hcc is decreased, further approaching the experimental one. Bulk solvent effect and explicit hydrogen bonds with water molecules affect in a similar way T(R)DA hcc's both from the qualitative (with the exception of the phenoxy oxygen atom) and the quantitative point of view. Interestingly, the presence of a "nonsymmetric" hydrogen bond with one water molecule does not cause any further "asymmetrization" of the phenoxy hcc's with respect to the "intrinsic" asymmetry due to the interaction with the peptide backbone. In summary, our calculations evidence that backbone−ring interactions remarkably influence both the conformational and the spectroscopic features of T(R)DA, suggesting that a dipeptide analogue is the simplest realistic model for the study of the magnetic properties of tyrosyl. Smaller molecules, such as *p*-ethylphenoxy, are probably too simple to reproduce the delicate balance of intraresidue interactions tuning the conformational and spectroscopic properties of tyrosine.

Acknowledgment. This work was supported by the Italian Research Council (CNR), by the Italian Ministry for the University and the Scientific and Technological Research (MIUR, grant 2001031717-005), and by the Gaussian, Inc. The technical support by the CIMCF (Centro Interdipartimentale di metodologie Chimico-Fisiche, Università Federico II) is also acknowledged.

JA020465K